INTERNATIONAL JOURNAL FOR NUMERICAL METHODS IN FLUIDS
Int. J. Numer. Meth. Fluids **28**: 617–631 (1998)

A FINITE ELEMENT ANALYSIS OF MACH REFLECTION BY USING THE BOUSSINESQ EQUATION

SHOICHIRO KATO[a,*,1], TOSHIMITSU TAKAGI[b,2] AND MUTSUTO KAWAHARA[c,3]

[a] *Technical Research Institute, OHKI Corporation, Chiba, Japan*
[b] *Department of Coastal Engineering, INA Corporation, Tokyo, Japan*
[c] *Department of Civil Engineering, Chuo University, 1-13-27 Kasuga, Bunkyo-ku, Tokyo 112, Japan*

SUMMARY

The numerical analysis of 'Mach reflection', which is the reflection of an obliquely incident solitary wave by a vertical wall, is presented. For the mathematical model of the analysis, the two-dimensional Boussinesq equation is used. In order to solve the equation in space, the finite element method based on the linear triangular element and the conventional Galerkin method is applied. The combination of explicit and semi-implicit schemes is employed for the time integration. Moreover, one of the treatments for the open boundary condition, in which the analytical solution of the linearized Boussinesq equation in the outside domain is linked to the discrete values of velocity and water elevation in the inside domain, is applied for the modeling of the Mach reflection problem. © 1998 John Wiley & Sons, Ltd.

KEY WORDS: Mach reflection; FEM; Boussinesq equation; open boundary; Miles' theory

1. INTRODUCTION

The prediction of wave propagation characteristics in the shallow water region is one of the most significant items for the prevention of the various hazards in the field of coastal engineering. However, the wave transformation in this region includes very complicated phenomena due to the simultaneous occurrence of several physical effects such as refraction, diffraction, reflection and so on. Besides, the finite amplitude wave theory must be introduced to predict these phenomena because the amplitude is relatively high in these areas. Therefore, the various kinds of wave propagation analysis based on the finite amplitude wave theory should be performed.

It is sometimes observed that the incident wave, with a certain incident angle, reflects with an extraordinarily high amplitude along the vertical wall. This phenomenon is known as the Mach reflection, which is studied in this paper. The previous observation [1] and experiments [2,3,10] had confirmed that ordinary reflection of a solitary wave by a vertical wall is impossible for adequately small angles of incidence and should be replaced by the Mach reflection. When it comes to be the Mach reflection, the apexes of the incident and the

* Correspondence to: Department of Civil Engineering, Chou University, 1-13-27 Kasuga, Bunkyo-ku, Tokyo 112, Japan.
[1] E-mail: giken@ohki.co.jp
[2] E-mail: takagi@indy2.civil.chuo-u.ac.jp
[3] E-mail: kawa@civil.chuo-u.ac.jp

CCC 0271–2091/98/140617–15$17.50

Received January 1996
Revised August 1996

reflected waves move away from the wall at a constant angle, and a third solitary wave, called the 'Mach stem', takes part at the wall. It is also reported that the reflected wave component vanishes according to the angle of incidence. This problem was also studied theoretically by Miles [4] as a special case of an oblique interaction of two small-amplitude solitary waves.

Recently, the numerical analysis of Mach reflection was performed by Funakoshi [5] and Tanaka [6]. Tanaka carried out this kind of calculation for a large-amplitude solitary wave and showed a certain comparison with the Miles' theory; the Miles' theory is based on the small-amplitude case. It should be considered that his research gave great contributions to coastal engineering. Against these, this paper reports on calculations by the finite element method (FEM) [7] and gives a comparison with the Miles' theory in the case of a small-amplitude incident wave. As the governing equation, the Boussinesq equation, which can estimate the effect of wave crest curvature to obtain more accurate results [9] against the assumption of hydrostatic pressure, is used for the non-linear dispersive wave analysis. A FEM to treat an arbitrary boundary configuration is utilized to solve the Boussinesq equation. A new treatment of the open boundary condition, which is one of the essential subjects in the numerical analysis of the wave propagation problem, is presented in this paper. To compute the Mach reflection appropriately, boundary problems which include such an open boundary should be investigated. Another purpose of this study is to perform adequate boundary treatments for the modeling of the Mach reflection problem.

2. GOVERNING EQUATIONS

Within a Cartesian co-ordinate system, the Boussinesq equation with two horizontal dimensions is introduced. The equations of motion and continuity can be described as

$$\frac{\partial u}{\partial t}+u\frac{\partial u}{\partial x}+v\frac{\partial u}{\partial y}+g\frac{\partial \eta}{\partial x}=\frac{h^2}{3}\left(\frac{\partial^3 u}{\partial x^2\,\partial t}+\frac{\partial^3 v}{\partial x\,\partial y\,\partial t}\right), \tag{1}$$

$$\frac{\partial v}{\partial t}+u\frac{\partial v}{\partial x}+v\frac{\partial v}{\partial y}+g\frac{\partial \eta}{\partial y}=\frac{h^2}{3}\left(\frac{\partial^3 v}{\partial y^2\,\partial t}+\frac{\partial^3 u}{\partial x\,\partial y\,\partial t}\right), \tag{2}$$

$$\frac{\partial \eta}{\partial t}+\frac{\partial}{\partial x}\{(h+\eta)u\}+\frac{\partial}{\partial y}\{(h+\eta)v\}=0, \tag{3}$$

where u and v denote velocity components for the x- and y-directions, respectively, and η, h and g represent wa&5vVvter elevation, water depth and gravity acceleration, respectively. The right-hand sides of Equations (1) and (2) denote the dispersion term in which the dynamic pressure can be complementarily estimated to obtain more-valid solutions against the assumption of the hydrostatic pressure. On the boundary S_1, the velocity is assumed as

$$u_n = ul = vm = \hat{u}_n \quad \text{on } S_1, \tag{4}$$

where $\hat{u}$ denotes the prescribed value on S_1 and the subscript n denotes a normal direction against this boundary. On the boundary S_2, the water elevation is specified as

$$\eta = \hat{\eta} \quad \text{on } S_2, \tag{5}$$

and on the open boundary S_3, the following continuity condition is imposed

$$u = \bar{u}, \qquad v = \bar{v}, \qquad \eta = \bar{\eta} \quad \text{on } S_3, \tag{6}$$

where the overbar relates to the prescribed values obtained by the solutions of the outer sea. The initial condition is

$$u = \hat{u}_0, \qquad v = \hat{v}_0, \qquad \eta = \hat{\eta}_0 \quad \text{at } t = 0, \tag{7}$$

where the overhat means the initial value at $t = 0$.

3. TREATMENT OF OPEN BOUNDARY

The treatment procedure for the open boundary condition is discussed in this section. The derivation of a linear solution on the open boundary is presented, considering a linkage between the inner and outer solutions. As mentioned before, the non-linear wave propagation inside domain (analytical domain) is considered, while the linear solution of the outer domain is assumed. So, if the wave with a large amplitude goes through the boundary from the inside domain to the outside domain, no proper boundary condition can be set because the outer solution assumed is not non-linear. However, this problem can be resolved by extending the analytical domain so that this non-conforming condition does not influence the analysis of the main parts. There is no essential resolution for the setting of the non-linear open boundary set. To consider such a boundary treatment in detail will be the subject of a future study.

The analytical solution is employed for the modeling of the outer sea. To do this, the linearized Boussinesq equation is used because of simplicity. The equations of motion and continuity are rewritten as

$$\frac{\partial u}{\partial t} + g\frac{\partial \eta}{\partial x} = \frac{h^2}{3}\left(\frac{\partial^3 u}{\partial x^2\,\partial t} + \frac{\partial^3 v}{\partial x\,\partial y\,\partial t}\right), \tag{8}$$

$$\frac{\partial v}{\partial t} + g\frac{\partial \eta}{\partial y} = \frac{h^2}{3}\left(\frac{\partial^3 v}{\partial y^2\,\partial t} + \frac{\partial^3 u}{\partial x\,\partial y\,\partial t}\right), \tag{9}$$

$$\frac{\partial \eta}{\partial t} + h\frac{\partial u}{\partial x} + h\frac{\partial v}{\partial y} = 0. \tag{10}$$

In order to derive the analytical solution, the velocity and water elevation are assumed in the following form

$$\bar{u} = \tilde{u}\,\exp(-j\omega t)\,\exp\{j(k_x x + k_y y)\}, \tag{11}$$

$$\bar{v} = \tilde{v}\,\exp(-j\omega t)\,\exp\{j(k_x x + k_y y)\}, \tag{12}$$

$$\bar{\eta} = \tilde{\eta}\,\exp(-j\omega t)\,\exp\{j(k_x x + k_y y)\}, \tag{13}$$

where $\tilde{u}$, $\tilde{v}$ and $\tilde{\eta}$ represent the amplitudes of velocity components and water elevation, respectively, and k_x, k_y, ω denote the components of wave numbers for the x- and y-directions and angular frequency, respectively. The following equation is obtained by substituting Equations (11)–(13) into Equations (8)–(10)

$$\begin{bmatrix} -A\omega & -C\omega & gk_x \\ -C\omega & -B\omega & gk_y \\ hk_x & hk_y & -\omega \end{bmatrix} \begin{bmatrix} \tilde{u} \\ \tilde{v} \\ \tilde{\eta} \end{bmatrix} = 0, \tag{14}$$

where

$$A = 1 + \frac{h^2}{3} k_x^2, \qquad B = 1 + \frac{h^2}{3} k_y^2, \qquad C = \frac{h^2}{3} k_x k_y.$$

The determinant of Equation (14) must be zero in order for $\tilde{u}$, $\tilde{v}$ and $\tilde{\eta}$ to have non-trivial solutions and can be derived as

$$\omega\{(AB - C^2)\omega^2 - gh(k_x^2 B + k_y^2 A - 2k_x k_y C)\} = 0. \tag{15}$$

The angular frequencies which satisfy Equation (15) are obtained as

$$\omega_1 = 0, \qquad \omega_2 = c\sqrt{\frac{k_x^2 B + k_y^2 A - 2k_x k_y C}{AB - C^2}}, \qquad \omega_3 = -c\sqrt{\frac{k_x^2 B + k_y^2 A - 2k_x k_y C}{AB - C^2}}, \tag{16}$$

where $c = \sqrt{gh}$ is wave velocity and ω_1, ω_2 and ω_3 denote angular frequencies of constant, outgoing and incident wave components, respectively. Substituting the general solutions into the linearized Boussinesq Equations (8)–(10), and assuming the outgoing waves (considering an angular frequency ω_2 only) to three directions (with three kinds of wave) through the open boundary, the following equation can be obtained

$$\begin{bmatrix} \bar{u} \\ \bar{v} \\ \bar{\eta} \end{bmatrix} = \sum_{n=1}^{3} \bar{\eta}_0^n \begin{bmatrix} \dfrac{g(k_x^n B^n - k_y^n C^n)}{\{A^n B^n - (C^n)^2\}\omega_2^n} \\ \dfrac{g(k_y^n A^n - k_x^n C^n)}{\{A^n B^n - (C^n)^2\}\omega_2^n} \\ 1 \end{bmatrix} \exp(-j\omega_2^n t)\exp\{j(k_x^n x + k_y^n y)\}, \tag{17}$$

where

$$\omega_2^n = c\sqrt{\frac{(k_x^n)^2 B^n + (k_y^n)^2 A^n - 2k_x^n k_y^n C^n}{A^n B^n - (C^n)^2}}$$

and $\bar{\eta}_0^n$ are unknown constants. Equation (17) can be applicable to the case when only the outgoing waves exist on the boundary; it is assumed that the constant and incident wave components do not exist. Wave number k at the open boundary can be determined by the wave period and velocity. Here the unknown constants in Equation (17) must be determined. This equation, which denotes the solution of the outside domain, can be presented in the following form

$$\bar{\phi}_\mu = W_{\mu\lambda}\bar{\eta}_0^\lambda \exp(-j\omega^\lambda t) \quad \mu, \lambda = 1,\ 2,\ 3. \tag{18}$$

On the other hand, the discrete values of velocity and water elevation of the inside domain are expressed in the following form

$$\phi_\mu = T_{\mu\gamma} w_\gamma, \tag{19}$$

where $\phi_\mu = (u,\ v,\ \eta)^T$, $w_\gamma = (u_\gamma,\ v_\gamma,\ \eta_\gamma)^T$, and $T_{\mu\gamma}$ denotes the coefficients of a linear interpolation function. In order to determine the unknown constants in Equation (18), the following continuity condition is applied to the open boundary

$$\int_{S_3} \phi_\mu^*(\phi_\mu - \bar{\phi}_\mu)\,\mathrm{d}S = 0, \tag{20}$$

where ϕ_μ^* denotes the weighting function. By substituting Equations (18) and (19) into

Equation (20), the unknown constants can be determined in the following form

$$\bar{\eta}_0^{\lambda} = W_{\mu\lambda}^{-1} T_{\mu\gamma} w_{\gamma} \exp(j\omega^{\lambda} t). \tag{21}$$

4. FINITE ELEMENT FORMULATIONS

To begin with, the governing Equations (1)–(3) are transformed into the following weighted residual equations by employing the conventional Galerkin method.

$$\int_{\Omega} u^* \frac{\partial u}{\partial t}\,\mathrm{d}\Omega + \frac{h^2}{3}\int_{\Omega} \frac{\partial u^*}{\partial x}\left(\frac{\partial^2 u}{\partial x\,\partial t} + \frac{\partial^2 v}{\partial y\,\partial t}\right)\mathrm{d}\Omega + \int_{\Omega} u^* u \frac{\partial u}{\partial x}\,\mathrm{d}\Omega + \int_{\Omega} u^* v \frac{\partial u}{\partial y}\,\mathrm{d}\Omega$$
$$+ g\int_{\Omega} u^* \frac{\partial \eta}{\partial x}\,\mathrm{d}\Omega = \frac{h^2}{3}\int_{S_3} u^*\left(\frac{\partial^2 \bar{u}}{\partial x\,\partial t} + \frac{\partial^2 \bar{v}}{\partial y\,\partial t}\right) n_x\,\mathrm{d}S, \tag{22}$$

$$\int_{\Omega} v^* \frac{\partial v}{\partial t}\,\mathrm{d}\Omega + \frac{h^2}{3}\int_{\Omega} \frac{\partial v^*}{\partial y}\left(\frac{\partial^2 v}{\partial y\,\partial t} + \frac{\partial^2 u}{\partial x\,\partial t}\right)\mathrm{d}\Omega + \int_{\Omega} v^* u \frac{\partial v}{\partial x}\,\mathrm{d}\Omega + \int_{\Omega} v^* v \frac{\partial u}{\partial y}\,\mathrm{d}\Omega$$
$$+ g\int_{\Omega} v^* \frac{\partial \eta}{\partial y}\,\mathrm{d}\Omega = \frac{h^2}{3}\int_{S_3} v^*\left(\frac{\partial^2 \bar{v}}{\partial y\,\partial t} + \frac{\partial^2 \bar{u}}{\partial x\,\partial t}\right) n_y\,\mathrm{d}S, \tag{23}$$

$$\int_{\Omega} \eta^* \frac{\partial \eta}{\partial t}\,\mathrm{d}\Omega + \int_{\Omega} \eta^* \frac{\partial (h+\eta)}{\partial x} u\,\mathrm{d}\Omega - \int_{\Omega} \frac{\partial \eta^*}{\partial x}(h+\eta)u\,\mathrm{d}\Omega + \int_{\Omega} \eta^* \frac{\partial (h+\eta)}{\partial y} v\,\mathrm{d}\Omega$$
$$- \int_{\Omega} \frac{\partial \eta^*}{\partial y}(h+\eta)v\,\mathrm{d}\Omega = -h\int_{S_3} \eta^*(\bar{u}n_x + \bar{v}n_y)\,\mathrm{d}S - \int_{S_3} \eta^*(\bar{u}n_x + \bar{v}n_y)\bar{\eta}\,\mathrm{d}S, \tag{24}$$

where u^*, v^* and η^* represent weighting functions for the velocity and the water elevation, respectively, and n_x, n_y denote the components of unit normals for the x- and y-directions. Applying the analytical solution which was derived in the last section to the right-hand side of Equations (22)–(24), and employing a linear interpolation function based on triangular finite elements, the finite element equations can be described in the following form

$$M_{\alpha\beta}\dot{u}_{\beta} + \frac{h^2}{3}(K_{\alpha x\beta x}\dot{u}_{\beta} + G_{\alpha x\beta y}\dot{v}_{\beta}) + L_{\alpha\beta\gamma x}u_{\beta}u_{\gamma} + I_{\alpha\beta\gamma y}v_{\beta}u_{\gamma} + gA_{\alpha\beta x}\eta_{\beta} - \frac{h^2}{3}D^{x}_{\alpha\mu}W^{-1}_{\mu\lambda}T_{\mu\gamma}w_{\gamma} = 0, \tag{25}$$

$$M_{\alpha\beta}\dot{v}_{\beta} + \frac{h^2}{3}(P_{\alpha y\beta y}\dot{v}_{\beta} + Q_{\alpha y\beta x}\dot{u}_{\beta}) + L_{\alpha\beta\gamma x}u_{\beta}v_{\gamma} + I_{\alpha\beta\gamma y}v_{\beta}v_{\gamma} + gZ_{\alpha\beta y}\eta_{\beta} - \frac{h^2}{3}D^{y}_{\alpha\mu}W^{-1}_{\mu\lambda}T_{\mu\gamma}w_{\gamma} = 0, \tag{26}$$

$$M_{\alpha\beta}\dot{\eta}_{\beta} + N_{\alpha\beta x\gamma}H_{\beta}u_{\gamma} - C_{\alpha x\beta\gamma}H_{\beta}u_{\gamma} + J_{\alpha\beta y\gamma}H_{\beta}v_{\gamma} - F_{\alpha y\beta\gamma}H_{\beta}v_{\gamma} + O^{\psi}_{\alpha\mu}W^{-1}_{\mu\lambda}T_{\mu\gamma}w_{\gamma}$$
$$+ Z^{\psi}_{\alpha\mu}(W^{-1}_{\mu\lambda}T_{\mu\gamma}w_{\gamma})^2 = 0, \tag{27}$$

where the overdot denotes differentiation with respect to time and the coefficient matrices can be expressed as follows

$$M_{\alpha\beta} = \int_{\Omega} \Phi_{\alpha}\Phi_{\beta}\,\mathrm{d}\Omega, \qquad K_{\alpha x\beta x} = \int_{\Omega} \Phi_{\alpha,x}\Phi_{\beta,x}\,\mathrm{d}\Omega, \qquad G_{\alpha x\beta y} = \int_{\Omega} \Phi_{\alpha,x}\Phi_{\beta,y}\,\mathrm{d}\Omega, \tag{28}$$

$$L_{\alpha\beta\gamma x}=\int_\Omega \Phi_\alpha\Phi_\beta\Phi_{\gamma,x}\,\mathrm{d}\Omega,\qquad I_{\alpha\beta\gamma y}=\int_\Omega \Phi_\alpha\Phi_\beta\Phi_{\gamma,y}\,\mathrm{d}\Omega,\qquad A_{\alpha\beta x}=\int_\Omega \Phi_\alpha\Phi_{\beta,x}\,\mathrm{d}\Omega, \tag{29}$$

$$P_{\alpha y\beta y}=\int_\Omega \Phi_{\alpha,y}\Phi_{\beta,y}\,\mathrm{d}\Omega,\qquad Q_{\alpha y\beta x}=\int_\Omega \Phi_{\alpha,y}\Phi_{\beta,x}\,\mathrm{d}\Omega,\qquad Z_{\alpha\beta y}=\int_\Omega \Phi_\alpha\Phi_{\beta,y}\,\mathrm{d}\Omega, \tag{30}$$

$$N_{\alpha\beta x\gamma}=\int_\Omega \Phi_\alpha\Phi_{\beta,x}\Phi_\gamma\,\mathrm{d}\Omega,\qquad J_{\alpha\beta y\gamma}=\int_\Omega \Phi_\alpha\Phi_{\beta,y}\Phi_\gamma\,\mathrm{d}\Omega,\qquad C_{\alpha x\beta\gamma}=\int_\Omega \Phi_{\alpha,x}\Phi_\beta\Phi_\gamma\,\mathrm{d}\Omega, \tag{31}$$

$$F_{\alpha y\beta\gamma}=\int_\Omega \Phi_{\alpha,y}\Phi_\beta\Phi_\gamma\,\mathrm{d}\Omega, \tag{32}$$

$$D^x_{\alpha\mu}=\frac{g}{D^\mu}\int_{S_3}\Phi_\alpha\,\mathrm{e}^{i(k^\mu_x x+k^\mu_x y)}\{(k^\mu_y)^2+(k^\mu_y)^2\}n_x\,\mathrm{d}S, \tag{33}$$

$$D^y_{\alpha\mu}=\frac{g}{D^\mu}\int_{S_3}\Phi_\alpha\,\mathrm{e}^{i(k^\mu_x x+k^\mu_y y)}\{(k^\mu_x)^2+(k^\mu_y)^2\}n_y\,\mathrm{d}S, \tag{34}$$

$$O^\psi_{\alpha\mu}=\frac{gh}{\omega^\mu_2 D^\mu}\int_{S_3}\Phi_\alpha\,\mathrm{e}^{i(k^\mu_x x+k^\mu_y y)}(k^\mu_x n_x+k^\mu_y n_y)\,\mathrm{d}S, \tag{35}$$

$$Z^\psi_{\alpha\mu}=\frac{g}{\omega^\mu_2 D^\mu}\int_{S_3}\Phi_\alpha\,\mathrm{e}^{2i(k^\mu_x x+k^\mu_y y)}(k^\mu_x n_x+k^\mu_y n_y)\,\mathrm{d}S, \tag{36}$$

where

$$D^\mu=1+\frac{h^2}{3}(k^\mu_x)^2+\frac{h^2}{3}(k^\mu_y)^2.$$

For the discretization in time, a one-step explicit scheme is used, which can be derived as follows

$$\left[M_{\alpha\beta}+\frac{h^2}{3}K_{\alpha x\beta x}\right]u^{n+1}+\left[\frac{h^2}{3}G_{\alpha x\beta y}\right]v^{n+1}=\left[M_{\alpha\beta}+\frac{h^2}{3}K_{\alpha x\beta x}\right]u^n+\left[\frac{h^2}{3}G_{\alpha x\beta y}\right]v^n$$
$$-\Delta t\left\{L_{\alpha\beta\gamma x}u^nu^n+I_{\alpha\beta\gamma y}v^nu^n+gA_{\alpha\beta x}\eta^{n+1}-\frac{h^2}{3}D^x_{\alpha\mu}W^{-1}_{\mu\lambda}T_{\mu\lambda}w^n_\gamma\right\}, \tag{37}$$

$$\left[M_{\alpha\beta}+\frac{h^2}{3}P_{\alpha y\beta y}\right]v^{n+1}+\left[\frac{h^2}{3}Q_{\alpha y\beta x}\right]u^{n+1}=\left[M_{\alpha\beta}+\frac{h^2}{3}P_{\alpha y\beta y}\right]v^n+\left[\frac{h^2}{3}Q_{\alpha y\beta x}\right]u^n$$
$$-\Delta t\left\{L_{\alpha\beta\gamma x}u^nv^n+I_{\alpha\beta\gamma y}v^nv^n+gZ_{\alpha\beta y}\eta^{n+1}-\frac{h^2}{3}D^y_{\alpha\mu}W^{-1}_{\mu\lambda}T_{\mu\lambda}w^n_\gamma\right\}, \tag{38}$$

$$\bar{M}_{\alpha\beta}\eta^{n+1}=\tilde{M}_{\alpha\beta}\eta^n-\Delta t\{N_{\alpha\beta x\gamma}H^nu^n-C_{\alpha x\beta\gamma}H^nu^n+J_{\alpha\beta y\gamma}H^nv^n-F_{\alpha y\beta\gamma}H^nv^n$$
$$+O^\psi_{\alpha\mu}W^{-1}_{\mu\lambda}T_{\mu\gamma}w^n_\gamma+Z^\psi_{\alpha\mu}(W^{-1}_{\eta\lambda}T_{\mu\gamma}w^n_\gamma)^2\}. \tag{39}$$

In Equation (39), $\bar{M}$ denotes the lumped coefficient of M, and $\tilde{M}$ is the mixed coefficient, which is written as

$$\tilde{M}=e\bar{M}+(1-e)M, \tag{40}$$

where e is referred to as the lumping parameter. Here, Equations (37) and (38) are solved using the element-by-element conjugate gradient method which is frequently used in numerical analysis of Navier–Stokes problems. Moreover, the equation of continuity (39) is solved before the equations of motion (37) and (38); these are solved using the water elevation at the $n+1$ time step.

5. NUMERICAL TEST FOR TREATMENT OF OPEN BOUNDARY

Before the analysis of the Mach reflection, an obliquely propagating solitary wave is analyzed to test the open boundary treatment. Figure 1 shows the finite element discretization in which the total number of nodes and elements are 10201 and 20000, respectively.

In this figure, the boundaries A–B and B–D are assumed to be open boundaries; the oblique incidence of a solitary wave is assumed on the boundaries A–C and C–D. The solitary wave on the incident boundary in this analysis is given by the first approximation of Laitone. Figure 2 shows the solitary wave propagation in one direction. The aspects at the vertical section B–C are shown in Figure 3. For the computational condition in this case, the lumping parameter is 0.9600 and the time increment is 0.0250 s. The incident wave height is 0.01 m, and the water depth is set at l.0 m. Moreover, the wave period for the determination of the wave number is assumed to be 20.0 s. The calculations represent a relatively good result for the treatment of the open boundary condition because the solitary wave is appropriately preserved in the propagation. It is considered that the treatment of the present scheme can be applicable to the outlet boundary in the Mach reflection analysis.

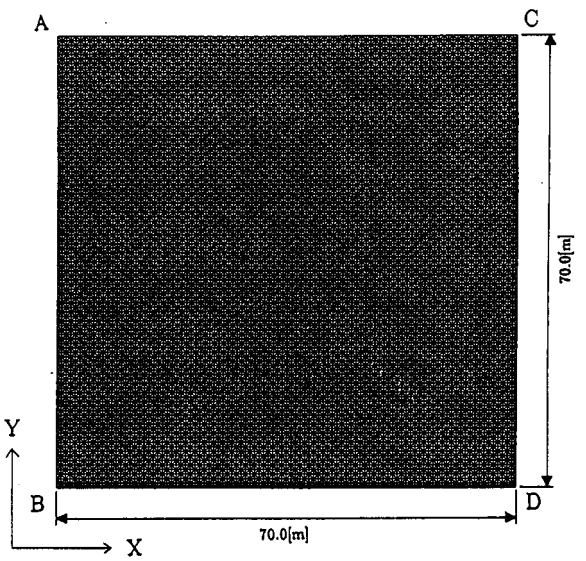

Figure 1. Finite element discretization.

6. MACH REFLECTION PROBLEM

6.1. Miles' theory

The main results with respect to the Mach reflection which were obtained by Miles, are briefly summarized in this section. Firstly, the symbol used in the following Miles' theory is defined. The amplitude of the incident wave divided by the still water depth h is represented by a_i, and ψ_i is the angle of incidence. Similarly, the amplitude of the reflected wave is denoted a_r, and ψ_r is the angle of reflection. Moreover, the amplitude of the Mach stem (or the maximum run-up at the wall) is defined as a_M, and ψ_* is the stem angle. The schematic representation of the Mach reflection problem is presented in Figure 4.

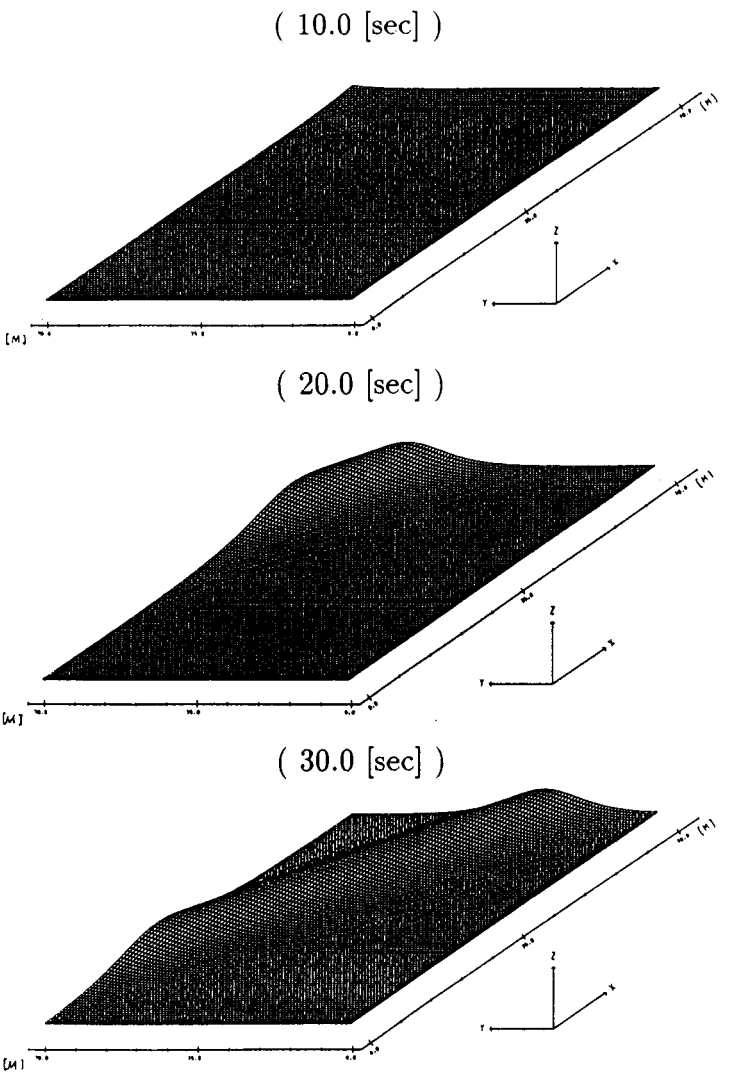

Figure 2. Solitary wave propagation.

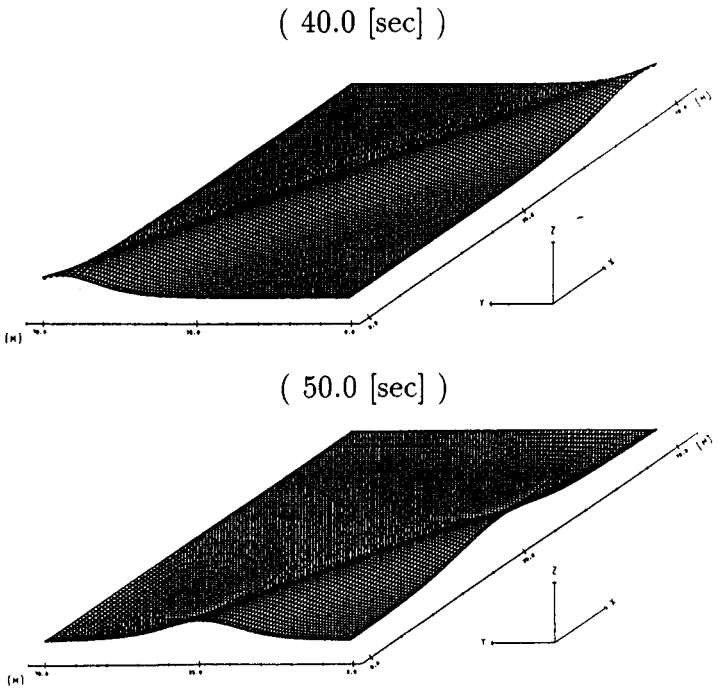

Figure 2 (*Continued*)

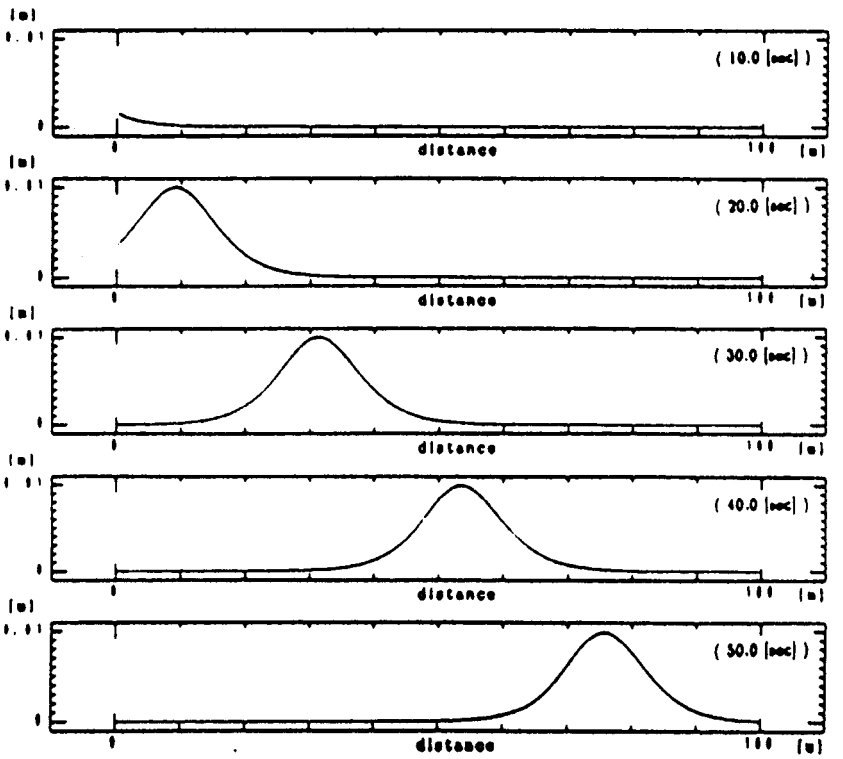

Figure 3. At section B–C.

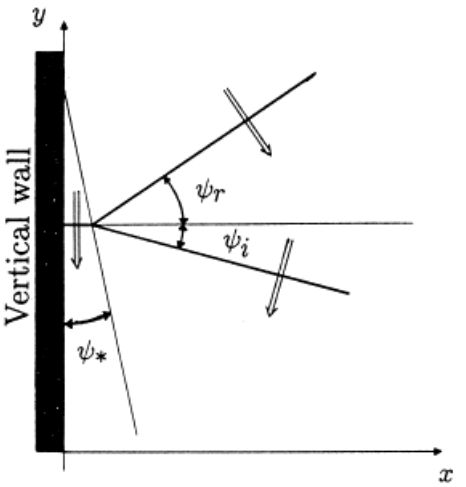

Figure 4. Definition sketch of Mach reflection problem.

According to the Miles' theory, which is based on the weak non-linearity, the regular type of reflection is changed into the Mach reflection when $a_i \ll 1$ and $\psi_i/(3a_i)^{1/2} \leq 1$. Then, ψ_r is not equivalent to ψ_i but has some larger value which depends on a_i. On the other hand, a_r is smaller than a_i and the reflected wave component vanishes according to ψ_i. Besides, Miles predicted that a_M becomes four-times of the incident amplitude when $\psi_i = (3a_i)^{1/2}$ and a steady solitary wave appears along the wall. The numerical simulation of the Mach reflection is performed and represented in the next section. A comparison, a_M/a_i versus ψ_i, is also carried out to confirm the quantitative agreement between the present calculation and the Miles' theory.

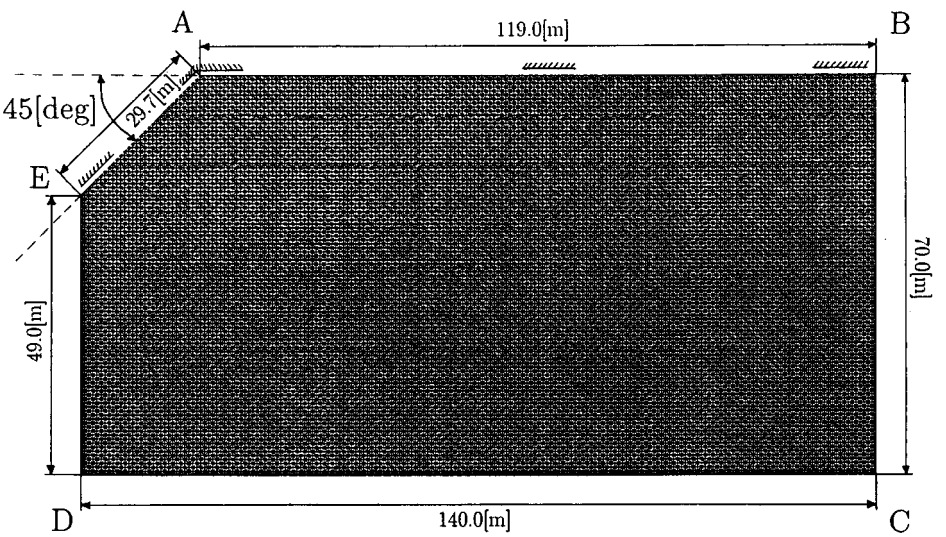

Figure 5. Finite element discretization for the Mach reflection.

6.2. Numerical tests

The solitary wave on the incident boundary is assumed by the first approximation solution of Laitone [8]

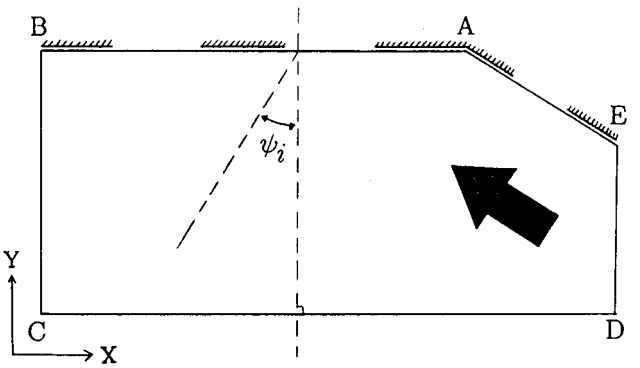

$$\eta = \eta_0 \operatorname{sech}^2 \sqrt{\frac{3\eta_0}{4h^3}}(x - ct + \alpha),$$

$$u = \sqrt{\frac{g}{h}}\,\eta\,\cos(\pi - \psi_i),$$

$$v = \sqrt{\frac{g}{h}}\,\eta\,\sin(\pi - \psi_i),$$

$$c = \sqrt{gh\left(1 + \frac{\eta_0}{h}\right)},$$

in which ψ_i represents the angle of incidence and α denotes a changeable distance. Figure 5 shows the finite element discretization in which the total number of nodes and elements are 19836 and 39100, respectively. In this figure, the boundary B–C is assumed to be an open boundary, and the oblique incidence of a solitary wave is assumed on the boundaries C–D and D–E. The boundaries A–B and A–E are assumed to be slip boundaries.

Figure 6 shows the pattern of Mach reflection, which was calculated at an incident angle of 45°. For the computational condition in this case, the lumping parameter and the time increment are the same as for the calculation of a solitary wave propagation.

The wave develops according to the time passed and it gradually becomes a steady state. Such a characteristic should be noted so as to estimate the correct value of the maximum run-up at the wall. The analytical domain should be extended along the wall line as far as possible. Therefore, about twice the length of the former mesh (Figure 1) is used. Figure 7 shows the time variation of velocity distribution, and the development of the phenomenon can be easily confirmed. For the computational condition, the incident wave height is 0.04 m and the angle of incidence is 20°.

A comparison between Miles' prediction and the present analysis, which is a_M/a_i versus ψ_i, is performed and shown in Figure 8. It should be noted that the Mach reflection is the initial value problem which depends on the incident amplitude and angle, and that it is in the ordinary process that the incident amplitude is fixed and the angle of incidence is varied. Here, the incident amplitude is 0.04 m and the increment of the angle is 5°. Moreover, the oblique wall is inclined in proportion to the angle of incidence so as to treat the incident boundary

adequately. A part of the mesh is deformed according to the angle of incidence. On the other hand, a_M/a_i according to ψ_i was described by Miles, e.g. there are three types of equation in this respect. One is the equation of the Mach reflection type, and the others are the equations of regular reflection type. The regular reflection types are grazing and non-grazing types. The difference between the two types has a relationship with the angle of interaction.

In Figure 8, the dot represent the computed results of the presented method, and the Miles' theory is described by the following Equations (a)–(c). Here, $\epsilon = \psi_i/(3a_i)^{1/2}$ is defined.

$$\frac{a_M}{a_i} = \begin{cases} (1+\epsilon)^2 \ldots \text{Mach reflection} & \text{(a)} \\ 4[1+(1-1/\epsilon^2)^{1/2}] \ldots \text{regular grazing reflection} & \text{(b)} \\ 2+[3/(2\sin^2\psi_i)-3+2\sin^2\psi_i]a_i \ldots \text{regular non}-\text{grazing reflection} & \text{(c)} \end{cases}$$

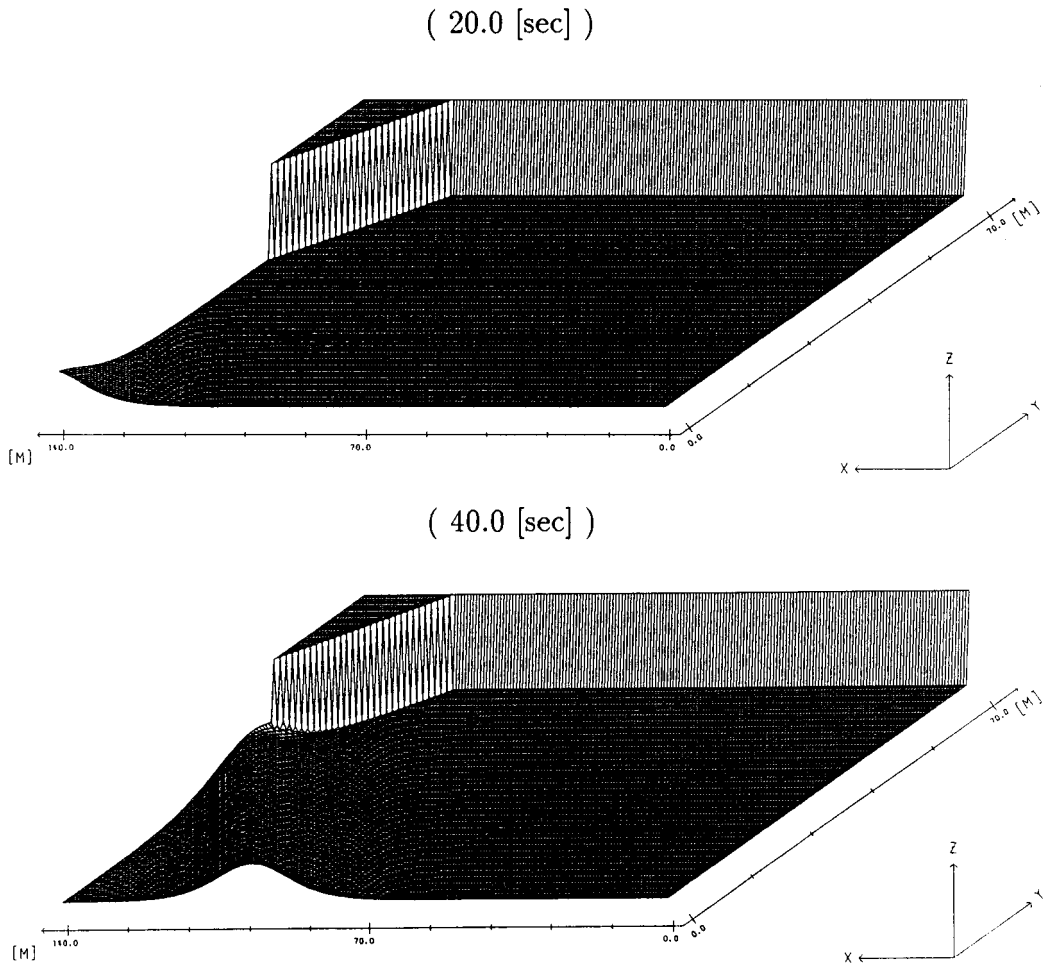

Figure 6. Mach reflection pattern computed by present scheme.

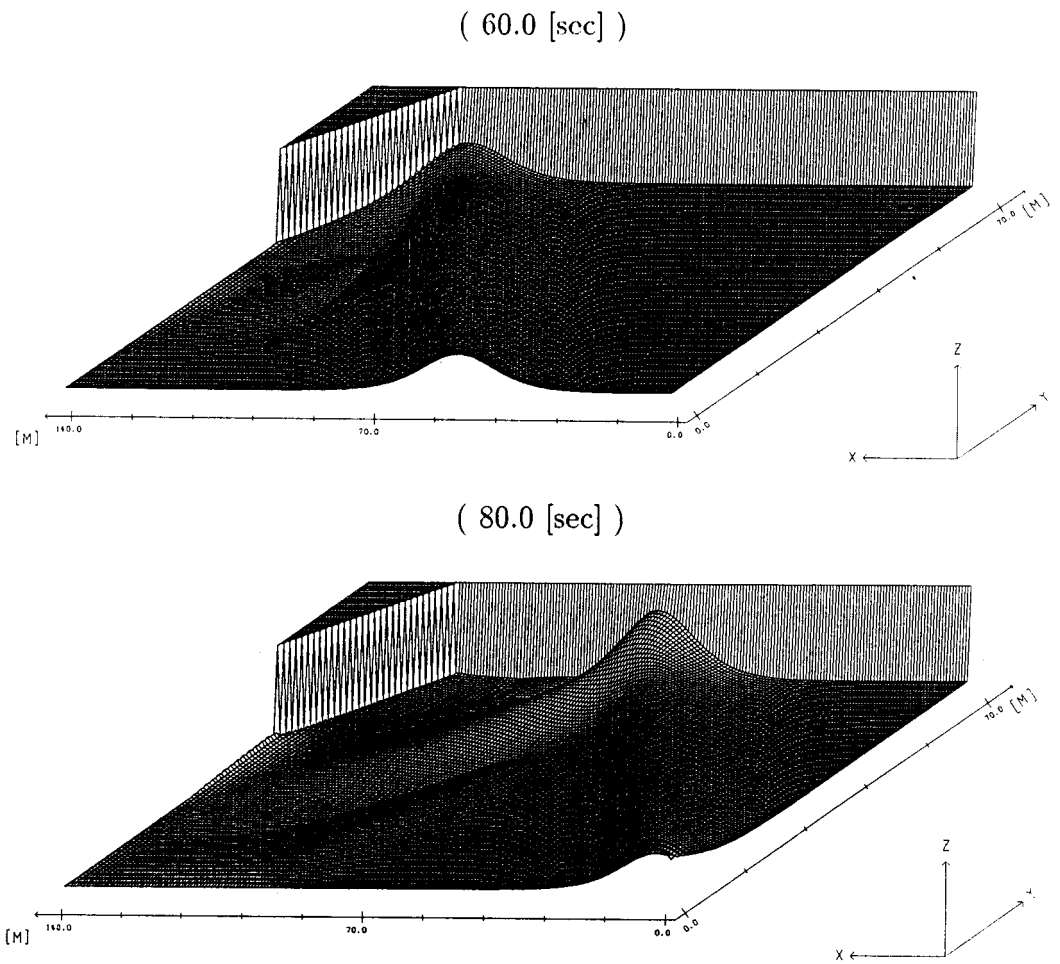

Figure 6 (*Continued*)

7. CONCLUSION

The finite element analysis of the Mach reflection with the open boundary is presented in this paper. The calculated results have shown qualitatively good agreements with the Miles' theory, and the existence of the Mach reflection has been reconfirmed. Quantitatively, there was also good agreement, as shown in Figure 8. For the small angle of incidence, the numerical maximum amplitude agrees with the analytical result of the Mach reflection type of Miles. It converges to the equation of the regular non-grazing type according to the angle enlarged. The treatment of the open boundary condition by the present scheme could be useful for the wave propagation problem. The treatment of the strong non-linearity and the extension of wave number components in the open boundary problem still remain as future subjects.

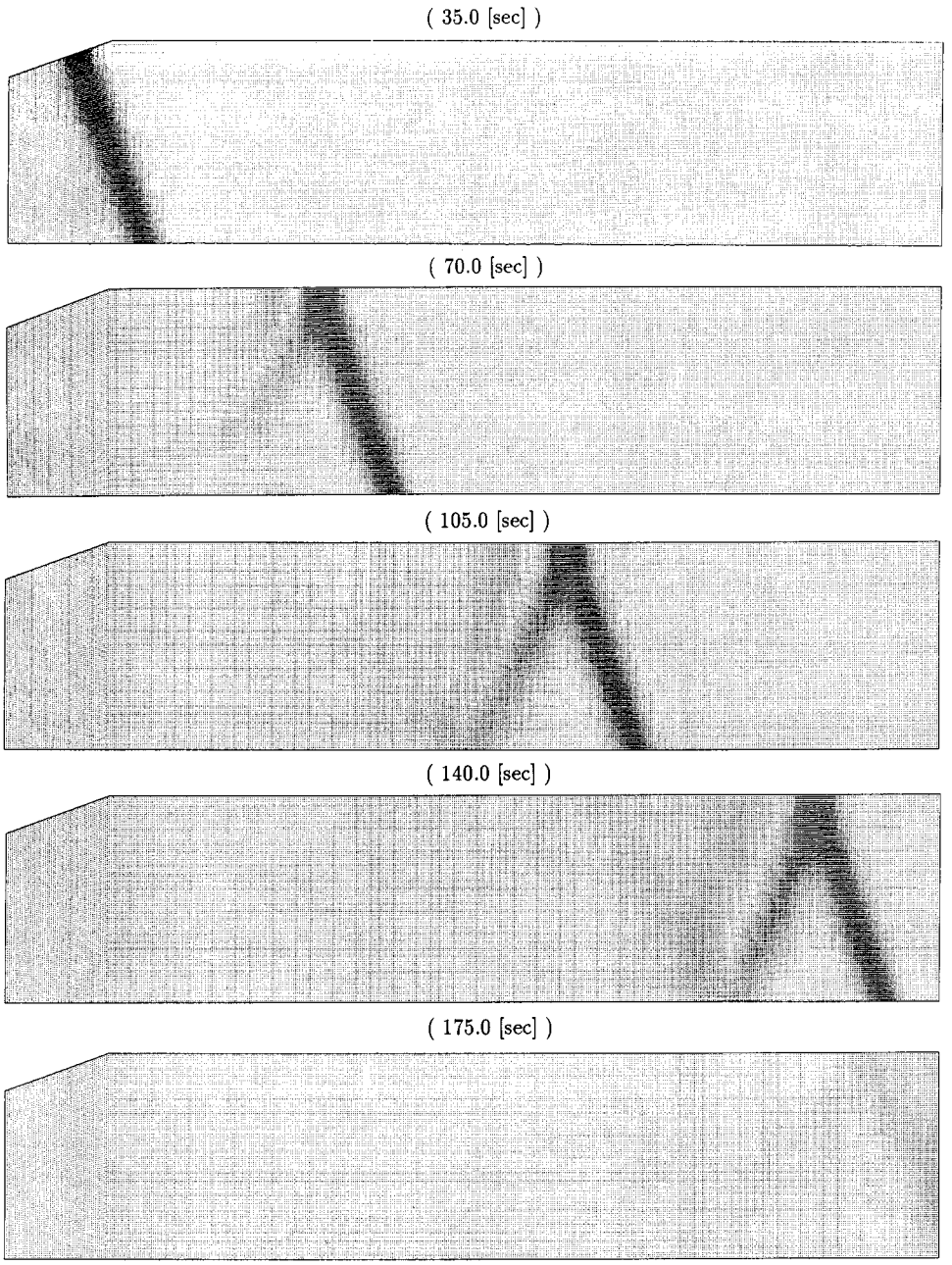

Figure 7. Time variation of velocity distribution.

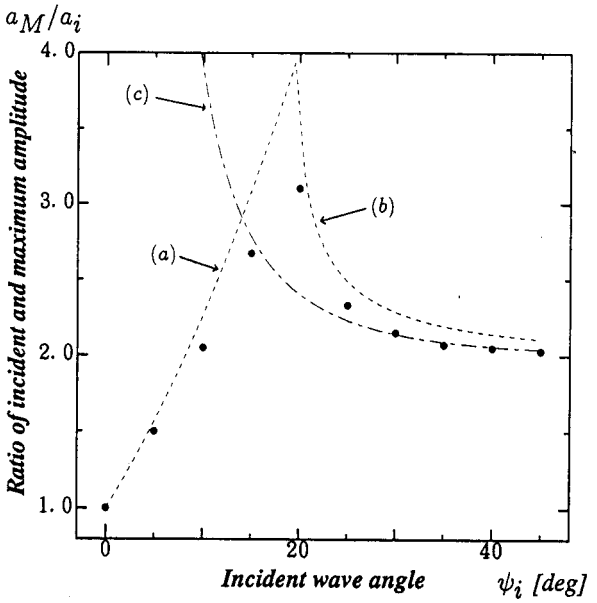

Figure 8. a_M/a_i vs. ψ_i.

REFERENCES

1. R.L. Wiegel, 'Water wave equivalent of Mach reflection', *Proc. 9th Conf. Coastal Eng.*, *ASCE*, Chap. 6, pp. 82–102, 1964.
2. P.H. Perroud, 'The solitary wave reflection along a straight vertical wall at oblique incidence', *Ph.D. Thesis*, University of California, Berkeley, CA, 1957.
3. T.C. Chen, 'Experimental study on the solitary wave reflection along a straight sloped wall at oblique angle of incidence', *US Beach Erosion Board Tech. Memo. No. 124*, 1961.
4. J.W. Miles, 'Resonantly interacting solitary waves', *J. Fluid Mech.*, **79**, 171–179 (1977).
5. M. Funakoshi, 'Reflection of obliquely incident solitary waves', *J. Phys. Soc. Jpn.*, **49**, 2371–2379 (1980).
6. M. Tanaka, 'Mach reflection of a large-amplitude solitary wave', *J. Fluid Mech.*, **248**, 637–661 (1993).
7. J.Y. Cheng and M. Kawahara, 'Study on finite element analysis of Boussinesq equation', *M.S. Thesis*, Chuo University, 1993.
8. E.V. Laitone, 'The second approximation to cnoidal and solitary waves', *J. Fluid Mech.*, **9**, 430–444 (1960).
9. D.H. Peregrine, 'Long waves on a beach', *J. Fluid Mech.*, **27**, S15–S27 (1967).
10. W.K. Melville, 'On the Mach reflexion of a solitary wave', *J. Fluid Mech.*, **98**, 285–297 (1980).

